We are IntechOpen, the world's leading publisher of Open Access books Built by scientists, for scientists

6,900
Open access books available

184,000
International authors and editors

200M
Downloads

Our authors are among the

154
Countries delivered to

TOP 1%
most cited scientists

12.2%
Contributors from top 500 universities



WEB OF SCIENCE™

Selection of our books indexed in the Book Citation Index in Web of Science™ Core Collection (BKCI)

Interested in publishing with us?
Contact book.department@intechopen.com

Numbers displayed above are based on latest data collected.
For more information visit www.intechopen.com



4

Role of Skeletal Muscle MRI in Peripheral Nerve Disorders

Nozomu Matsuda, Shunsuke Kobayashi and Yoshikazu Ugawa
Fukushima Medical University, Department of Neurology
Japan

1. Introduction

In diagnosing peripheral nerve disorders, the involved nerves can usually be determined based on clinical history and neurological findings with the aid of electrophysiological examinations. Despite the principle, we often encounter diagnostic challenges. In this chapter, we describe the clinical utility of magnetic resonance imaging (MRI) for the evaluation of peripheral nerve disorders. MRI can visualize pathological changes in skeletal muscles secondary to lesions of the peripheral nerve, plexus or nerve root. The lesion sites may be inferred based on the distribution of the involved muscles.

After the first report in 1987 (Shabas et al., 1987), MRI has increasingly been used to evaluate denervated muscles (West et al., 1994; Fleckenstein et al., 1993; Uetani et al., 1993). In particular, studies of entrapment or compressive neuropathy have greatly contributed to the understanding of clinical-radiological correlations in peripheral nerve damage. Animal experiments have also been conducted, in which muscle MRI was examined after peripheral nerve transection.

MRI has several distinct advantages over needle electromyography (EMG), including non-invasiveness, accessibility to deep muscles and interexaminer reliability (Koltzenburg and Bendszus, 2004; Bendszus et al., 2003; McDonald et al., 2000). MRI is particularly useful as needle EMG is difficult to perform on children or patients on anticoagulation. Excellent spatial resolution allows MRI to detect atrophy of the small muscles, moreover, different MRI pulse sequences show sensitivity to different stages of denervation, thus, MRI can provide valuable information about the duration of muscle denervation (Kamath et al., 2008). MRI has a potential to visualize mass lesions causing nerve damage, such as tumours, which is useful for the clinical judgment of surgical resectability (Grant et al., 2002).

An abnormal MR signal in muscles is not specific to denervation and may also be seen in any condition that causes muscle edema, including severe muscle strains, blunt trauma and acute myositis. Thus, MRI findings need to be interpreted in combination with other clinical information. Previous muscle MRI studies of peripheral nerve disorders have mostly focused on entrapment or compression neuropathy (Andreisek et al., 2006; Petchprapa et al., 2010; Donovan et al., 2010). However, given its capability in visualizing pathological changes and mapping the distributions of the involved muscles, the use of MRI can be extended to a variety of peripheral nerve disorders. We will give a theoretical background of muscle MRI and describe its clinical applications in peripheral nerve disorders with some representative cases. We will also mention non-muscular features of MRI, e.g. nerve signal

and mass lesions causing nerve damage, which contribute to the diagnosis of peripheral nerve disorders.

2. Radiological basis of muscle MRI

Normal muscles have intermediate to long T1 and short T2 relaxation times of MRI relative to the surrounding soft tissue. The spin-echo decay curve of skeletal muscle has been modelled to fit into a multi-exponent curve, in which the longer component is extracellular water and the shorter component is intracellular water (Hazlewood et al., 1974). The other determinants of MR relaxation times in muscle include tissue fat, total water content and blood volume. In theory, increased extracellular fluid in denervated muscles causes prolongation of both T1 and T2 relaxation times, because the relaxation time of water in the extracellular space of muscle is about four times that of the myoplasm (Polak et al., 1988). Most clinical studies show a normal T1 signal in the denervated muscles in the acute phase, thus sensitivity of the T1-weighted sequence appears to be low for detection of early stage denervation. By contrast, T2-weighted images reliably detect muscle denervation in the acute phase. A longitudinal imaging study in rats showed T2 signal changes as early as 48 hours after complete transection of the sciatic nerve and the signal intensity continued to increase until two months after denervation (Bendszus et al., 2002; Table 1).

Another factor that may contribute to MRI signal changes in denervated muscles is the altered blood flow caused by an interruption of the sympathetic vasoconstriction. Blood flow increases immediately after denervation, with a subsequent decline in the following week. An experimental nerve compression study found a strong correlation between T2 signal intensity and blood volume *in vivo* (Hayashi et al., 1997; Wessig et al., 2004). However, the time course of the blood flow changes was not in parallel to that of the MR signal changes. Thus, it remains unclear as to how much the blood flow changes explain MR signals in denervated muscles.

Several MR sequences are known to be particularly sensitive to early changes in denervated muscles. Inversion-recovery imaging, including turbo inversion recovery magnitude (TIRM) and short tau inversion recovery (STIR), suppresses the fat signal based on differences in the T1 relaxation time of the tissues and enhances differences between the water content of the tissues. In an experimental nerve transection study with rats, the TIRM signal started to increase as early as 24 hours after denervation (Bendszus et al., 2002). In clinical studies, an abnormal STIR signal in the denervated muscles has been demonstrated within four days after the onset of clinical symptoms (West et al., 1994). Generally, the threshold for producing an increased STIR signal is weakness graded at '3' (antigravity) or less out of '5' on the Medical Research Council's (MRC) scale.

Use of a contrast medium, such as gadolinium (Gd) diethyltriaminepentaacetic acid, may increase sensitivity for detecting muscle denervation. Gd uptake appears to start within days after symptom onset and the extent of the enhancement correlates with electrophysiological signs of denervation. A rat experiment showed the Gd enhancement as early as 24 hours after nerve lesion and the effect increased over time until it reached a plateau on day 21 (Bendszus and Koltzenburg, 2001). Gd enhancement could be caused by a dilatation of the vascular bed, an enlargement of the extracellular space or both. Therefore, fluid accumulation appears to contribute to both Gd uptake and T2 prolongation.

Traditionally, nerve injury is classified into three grades. In neurapraxic nerve injuries, axons are spared but myelin sheath is damaged causing conduction delay or block. The

damage is usually transient and self-limiting with complete recovery. Axonotmesis is the intermediate grade of nerve injury, in which axons distal to the site of injury are disrupted with preserved connective tissue framework of the nerve. Neurotmesis is the most severe form of nerve injury, characterized by loss of axonal continuity along with disruption of the surrounding myelin sheath and connective tissue. The aforementioned signal changes in T2, TIRM and STIR sequences are observed in severe axonotmetic and neurotmetric injuries, in which the axons are disrupted and Wallerian degeneration follows. In axonotmetic nerve injuries, the abnormal signal of muscle MRI will return to normal as axons regenerate (Kikuchi et al., 2003). In neurotmetic injuries, the increased MR signal in the involved muscles will eventually decrease with atrophy and fatty infiltration, which is best visualized with the T1-weighted sequence. MRI may be able to differentiate axonotmetic from neurotmetic nerve injury, because the increased T2 signal persists longer in neurotmesis than in axonotmesis. In predominantly neurapraxic injuries with minimal axonal loss, the involved muscles exhibit normal signal characteristics on T2 and STIR pulse sequences.

	T1-weighted	T2-weighted	STIR	Gadolinium
Acute (< 1 month)	Unchanged	Increased	Increased	Enhancement
Subacute (1-6 months)	Unchanged	Increased	Increased or Normalized	No enhancement
Chronic (> 6 months)	Increased (fatty degeneration) or Unchanged (fair reinnervation)	Increased or Normalized	Normalized	No enhancement

Table 1. MRI findings of denervated muscles at different stages.

3. Correlations between muscle MRI and electrophysiological findings

The EMG findings in peripheral nerve disorders reflect the functional processes of denervation and reinnervation. Active denervation causes spontaneous discharge of single muscle fibres, which is observed as fibrillation potentials and positive sharp waves. Spontaneous motor unit potentials caused by irritability of motor neurons are observed as fasciculation. In the case of traumatic nerve injuries, EMG evidence of denervation usually develops in two to three weeks. On the other hand, early change of MRI signal in denervated muscles is observed as early as four days after the onset of clinical symptoms (West et al., 1994). Thus, MRI signal change appears to develop no later than EMG change. Good time sensitivity of MRI may reflect early development of the myoplasm-to-extracellular fluid shift in denervated muscles as compared with delayed electrophysiological manifestation of spontaneous EMG activity.

Beside the time sensitivity, detection sensitivity is also important when considering radiological-physiological correlations. McDonald and colleagues directly compared the findings of MRI and needle EMG in 90 patients with peripheral nerve injury or radiculopathy of one to four months duration (McDonald et al., 2000). The results of the two

methods matched anatomically in 49 subjects, i.e. the specific muscles showing abnormal spontaneous EMG activity correlated directly with the increased STIR signal on MRI. Moreover, the STIR intensity tended to increase with the higher degree of spontaneous activity as measured with EMG. It should be noted that, in 16 (18%) subjects, abnormal spontaneous EMG activity was present in the muscles that did not show increased STIR. The results indicate that the STIR has lower sensitivity than needle EMG. Bendszus and colleagues conducted a similar study with Gd-enhanced MRI in patients with a foot drop caused by L5 radiculopathy, common peroneal nerve palsy and sciatic nerve palsy. They found that Gd enhancement was more prominent in the muscles with EMG signs of denervation compared to those without denervation signs (Bendszus and Koltzenburg, 2001; Bendszus et al., 2003). To summarise, the STIR and Gd-enhanced MRI have good sensitivity for detecting denervated muscles, if not better than needle EMG.

After acute denervation, reinnervation occurs by collateral sprouting, which manifests on EMG as polyphasic motor unit action potentials (MUPs) with a prolonged duration. During the chronic stage, reinnervated muscle fibres are integrated into large MUPs. In a study that examined EMG and MRI in patients with axonal motor sensory polyneuropathy, the MUP size showed a positive correlation with T1 signal intensity. Thus, the increase of T1 signal may well reflect the fatty replacement of those muscle fibres that are not reinnervated and thus not integrated into working motor units (Jonas et al., 2000).

4. Basics of peripheral nerve imaging

The standard evaluation of a peripheral nerve is based on morphological image analysis on T1-weighted sequences and on signal change analysis on fat-suppressed sequences. T2-weighted images have exquisite resolution, but pathologic findings are generally not as conspicuous as on STIR imaging. Normal peripheral nerves appear isointense compared to muscle, surrounded by a small rim of fat tissue. An entrapped nerve generally shows increased signal on T2-weighted and STIR images over the abnormal segment (Hof et al., 2008; Stoll et al., 2009; Thawait et al., 2011; Table 2). Distal extension of the high intensity signal in an injured nerve may indicate axonal damage due to Wallerian degeneration.

	Normal peripheral nerve	Abnormal peripheral nerve
Size	Smaller than accompanying artery	Larger than accompanying artery Focal or diffuse enlargement
Fascicular pattern	Seen in especially large nerves	Loss of normal fascicular pattern
T1-weighted	Isointensity to muscle	Isointensity to muscle
T2-weighted	Iso to minimal high intensity	Moderate to marked high intensity
Gadolinium	No enhancement	Enhancement (when blood-nerve barrier is disturbed)

Table 2. MRI findings of a normal and abnormal peripheral nerve (modified from Thawait et al., 2011 with permission).

The signal changes of injured nerves on T2-weighted and STIR images may reflect changes in water content due to altered axoplasmic flow, endoneurial or perineurial edema as a result of changes in the blood-nerve barrier or axonal myelin degeneration (Filler et al., 1996).

5. Clinical application of MRI in peripheral nerve disorders

MRI has been used to detect mass lesions and inflammation causing entrapment or compression neuropathy. MRI can also evaluate muscle denervation secondary to nerve damage. Thus it is applied to a wide range of peripheral nerve disorders, including polyneuropathy, radiculopathy and plexopathy. MRI may show a specific pattern of denervated muscles depending on the level of peripheral nerve damage. Here we describe the MRI findings of common peripheral nerve disorders and discuss the clinical utility of MRI.

5.1 Mononeuropathy

The common causes of mononeuropathy include entrapment, compression and stretch of the nerves. Nerve entrapment often occurs at the sites where the nerve courses through fibro-osseous or fibromuscular tunnels or penetrates a muscle. Nerve compression may be due to an adjacent mass, such as ganglion, synovial cyst, lipoma and tumour. Inflammation from tenosynovitis and bursitis may also cause mononeuropathy. It is clinically important to determine the lesion sites and evaluate the severity and prognosis. MRI is useful for the diagnosis of mononeuropathy because: i) a mass lesion causing nerve compression may be directly depicted, ii) a localized abnormal T2 signal may be seen within the injured segment of the nerves, and iii) involved muscles may show an abnormal MR signal, indicating the severity and duration of denervation. This section focuses on common types of mononeuropathy with special emphasis on MRI findings (Sallomi et al., 1998; Lisle and Johnstone, 2007; Kim et al., 2011).

5.1.1 Median nerve

Carpal tunnel syndrome (CTS) is the most common entrapment neuropathy. CTS presents with intermittent pain and numbness of the thumb, index, middle and radial half of the ring finger. Long-standing CTS leads to weakness and atrophy of the abductor pollicis brevis, opponens pollicis, flexor pollicis brevis and the first and second lumbrical muscles. Occasionally, sensory symptoms of the CTS may present beyond the median nerve territory, sometimes mimicking radicular pain in cervical radiculopathy. Differential diagnosis of CTS includes C6-7 radiculopathy, polyneuropathy and proximal entrapment of the median nerve. Electrodiagnostic tests are 85-90% accurate in patients with CTS, with a false-negative rate of 10-15%. Therefore, in cases of clinically symptomatic CTS with normal electrophysiological findings, MRI has a complementary role in diagnosis. The denervated thenar muscle may show an increased STIR signal (West et al., 1994; Jarvik et al., 2002). It has been reported that the median nerve itself shows an abnormal MRI signal in CTS. The common findings are isolated prestenotic and intracarpal swelling and an increased T2 signal retrograde to the distal radius (Mesgarzadeh et al., 1989). Anatomical constriction of the median nerve may also be revealed by MRI. Pronounced palmar bowing of the flexor retinaculum (transverse carpal ligament) observed in the MRI

of CTS patients show a significant correlation with subjective reports of pain severity (Tsujii et al., 2009). Horch and colleagues conducted a dynamic MRI study of 20 wrists of CTS patients (Horch et al., 1997). They measured the cross-sectional area of the carpal tunnel with different angles of wrist flexion and extension. They demonstrated that the carpal tunnel was smaller during wrist flexion, but the size was not significantly smaller in CTS patients as compared with normal volunteers. They also conducted a longitudinal study of CTS after surgical decompression. They found that the distal flattening of the median nerve, as visualized by MRI, normalized in 94% of the patients and the abnormal T2 signal decreased in 67% of the patients within six months postoperatively. Jarvik and colleagues prospectively studied a large cohort of 120 subjects with clinically suspected CTS (Jarvik et al., 2002). They checked five MRI parameters, namely median nerve signal, degree of nerve compression, bowing of the flexor retinaculum, thickening of the flexor tendon interspace and thenar muscle signal. An increased median nerve signal in the STIR sequence had a high sensitivity (88%), but specificity was low (39%). By contrast, an increased thenar muscle signal had a low sensitivity (10%), but specificity was high (90%). A combination of all parameters yielded high sensitivity (92%), but specificity was low (39%). To recap, electrophysiological tests are still the gold standard, but MRI plays a complementary role in the diagnosis of CTS.

The anterior interosseous nerve is the largest branch of the median nerve, innervating the flexor pollicis longus (FPL), pronator quadratus and the radial half of the flexor digitorum profundus (FDP) muscles. Anterior interosseous nerve syndrome, also known as Kiloh-Nevin syndrome, is usually caused by entrapment or compression of the median nerve in the proximal forearm. The patients show pinching deformity due to weakness of the FPL or FDP muscle. Because the anterior interosseous nerve is purely a motor nerve, its damage will not cause sensory loss, though dull pain may be present in the volar aspect of the forearm. During the acute to subacute stages, axial T2 or STIR images may depict a high intensity signal in the FPL, FDP and pronator quadratus muscles (Grainger et al., 1998; Spratt et al., 2002). However, the MRI findings have to be interpreted carefully, because a recent study showed that high intensity in the pronator quadratus muscle is sometimes observed in subjects without evidence of anterior interosseous nerve syndrome (Gyftopoulos et al., 2010). Over diagnosis of the anterior interosseous nerve syndrome should be avoided by knowing the prevalence of increased MR signals in the pronator quadratus muscle.

5.1.2 Ulnar nerve

The cubital tunnel, located posterior to the medial epicondyle of the humerus, is the most common site of ulnar nerve palsy. The possible causes of cubital tunnel syndrome include external compression (e.g. sleep palsy, perioperative damage), prolonged and excessive elbow flexion, trauma (e.g. from using jackhammers, humeral fracture with loose bodies or callus formation), a nerve-compressing lesion (e.g. ganglionic cysts, lipoma) and infection (Kato et al., 2002). Clinically, cubital tunnel syndrome presents with weakness and atrophy of hand intrinsic muscles, and sensory loss at the ring and little fingers. The MRI shows high intensity signals with a T2-weighted or STIR pulse sequence in the flexor carpi ulnaris and the ulnar half of the FDP muscles. Dynamic compression and inflammation will be seen on MRI as thickening and high intensity of the ulnar nerve on sagittal T2-weighted images (Rosenberg et al., 1993). Compression by a soft tissue mass may also be well depicted with

MRI. Dislocation and subluxation of the ulnar nerve would be detected on axial images during elbow flexion.

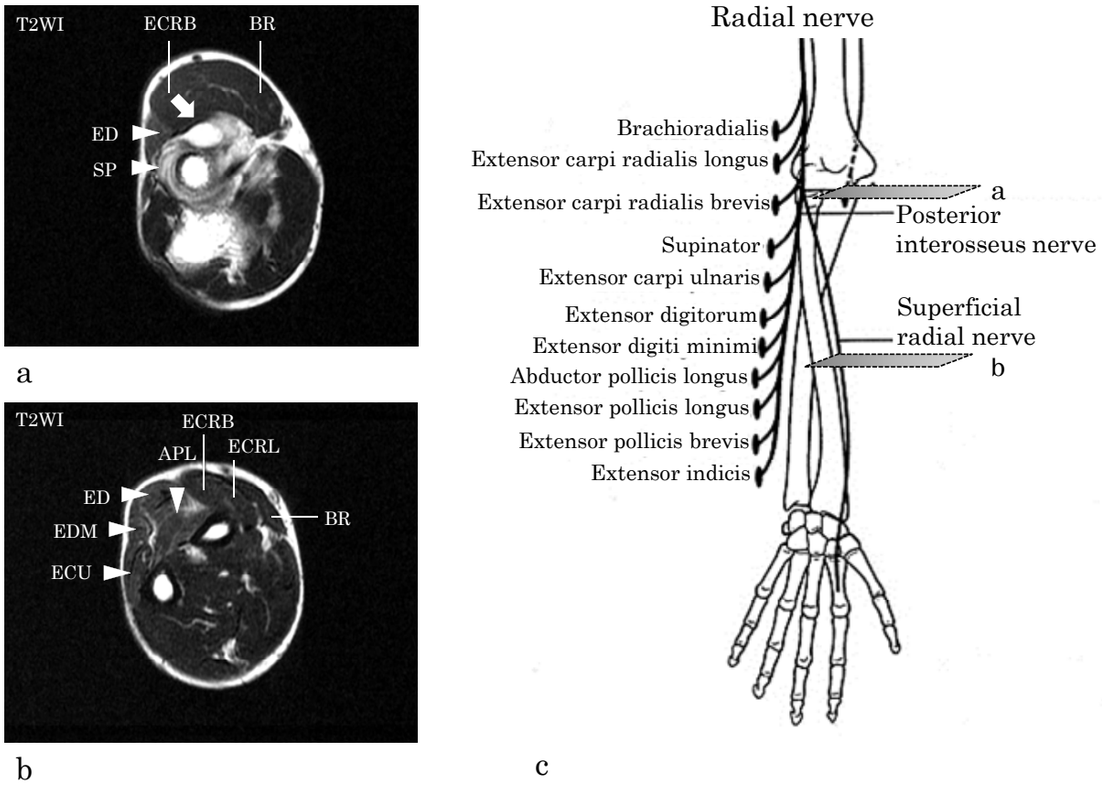
Guyon canal syndrome results from entrapment of the ulnar nerve as it passes through the wrist. Possible causes of ulnar nerve lesions at the Guyon canal include cystic lesions and chronic repetitive trauma (e.g. handlebar palsy in cyclists). Patients of Guyon canal syndrome experience wrist pain, sensory deficit in the ulnar nerve territory and weakness of ulnar intrinsic hand muscles. The hypothenar muscle may be spared in a distal lesion of the deep motor branch. A MRI may help exclude the presence of a mass lesion (Pearce et al., 2009) and an axial MRI at the level of the metacarpal bones is useful for detecting denervation of the intrinsic hand muscles (Andreisek et al., 2006).

5.1.3 Radial nerve

Radial tunnel syndrome (also known as posterior interosseous nerve syndrome or supinator (SP) muscle syndrome) is caused by entrapment or compression of the deep branch of the radial nerve, as it passes under the tendinous arch of the supinator muscle (arcade of Frohse). The posterior interosseous nerve supplies the extensor carpi ulnaris (ECU) muscle and the digital extensor muscles. The most consistent symptoms are deep aching pain in the forearm, pain radiation to the neck and shoulder, a sense of heaviness of the affected arm and an inability to sleep on the affected side (Rinker et al., 2004). Frequent causes of this syndrome are trauma, tumours, bursitis and cysts. Differential diagnoses include lateral epicondylitis (tennis elbow) and cervical radiculopathy. Electrophysiological studies are not useful in confirming the diagnosis, because the results are often normal or equivocal and no well-established criteria for diagnosis exist. MRI is useful to screen for a mass lesion compressing the posterior interosseous nerve. MRI may also detect denervation signals in the muscles supplied by the posterior interosseous nerve. Ferdinand and colleagues retrospectively studied 25 patients who were clinically suspected of having radial tunnel syndrome (Ferdinand et al., 2006). The most common MRI finding was denervation edema within the muscles innervated by the posterior interosseous nerve, most frequently within the SP (44%) and less frequently within the proximal forearm extensor muscles (12%). Seven patients (28%) showed evidence of a mass effect along the course of the posterior interosseous nerve, including thickening of the leading edge of the extensor carpi radialis brevis, prominent recurrent radial vessels, a schwannoma and a bicipitoradial bursa.

Case Presentation: Posterior interosseus nerve palsy

A 57-year-old male farmer noticed weakness of the right fingers after harvesting rice. Neurological examination revealed isolated finger extensor weakness 2/5 MRC scale with no sensory deficits. Deep tendon reflexes were normal. A painless mass was palpable in the right proximal forearm. The EMG showed active neurogenic change in the right extensor digitorum communis muscle. An MRI study detected a cystic lesion in the proximal forearm (Fig. 1a, arrow). The T2 high signal was observed in the radial-innervated muscles distal to the extensor carpi radialis brevis (ECRB) muscle (SP, ECU, extensor digitorum [ED], extensor digitorum minimi and abductor pollicis longus [APL] muscles in Fig. 1a, 1b, arrowheads). The signal was normal in the ECRB and brachioradialis (BR) muscles, which are innervated by branches of the radial nerve proximal to the posterior interosseous nerve. The pattern of the denervated muscles was compatible with the diagnosis of posterior interosseous nerve palsy caused by compression around the radial tunnel.



Abbreviations: abductor pollicis longus (APL), brachioradialis (BR), extensor carpi radialis brevis (ECRB), extensor carpi radialis longus (ECRL), extensor carpi ulnaris (ECU), extensor digitorum (ED), extensor digitorum minimi (EDM), supinator (SP).

Fig. 1. A case of radial tunnel syndrome caused by a cystic mass. (a, b) Axial T2-weighted MRI of the right forearm. (c) Schema of the radial nerve branches. The planes designated a and b in (c) correspond to the axial slice positions of (a) and (b), respectively.

5.1.4 Common peroneal nerve

Common peroneal nerve palsy is the most common mononeuropathy in the lower extremities. Its major cause is trauma, such as compression or stretch at the fibular neck, where the nerve is superficial and vulnerable to injury. The common peroneal nerve bifurcates into the superficial and deep peroneal nerves below the fibular neck. The superficial peroneal nerve supplies the peroneus longus (PL) and brevis muscles, and the deep peroneal nerve supplies the tibialis anterior (TA), extensor digitorum longus (EDL) and extensor hallucis longus muscles. Because both superficial and deep branches of the peroneal nerve innervate foot dorsiflexor muscles, foot drop is caused by damage to either branch. MRI may indicate specific sites of peroneal nerve damage: denervation limited in the anterior compartment (TA and EDL) or lateral compartment (PL) muscles indicates damage of the deep or superficial peroneal nerve, respectively. Involvement of the muscles in both anterior and lateral compartments (TA, EDL and PL) indicates a more proximal lesion of the common peroneal nerve. MRI may also be useful to detect mass lesions, such as ganglion, synovial cyst and osseous mass in a non-traumatic peroneal nerve (Iverson, 2005; Kim et al., 2007). The patterns of muscle denervation observed on MRI may also help

distinguish peroneal nerve palsy from sciatic nerve palsy, L5 radiculopathy and lumbosacral plexopathy (Bendszus and Koltzenburg, 2001; Bendszus et al., 2003; see also section 5.2).

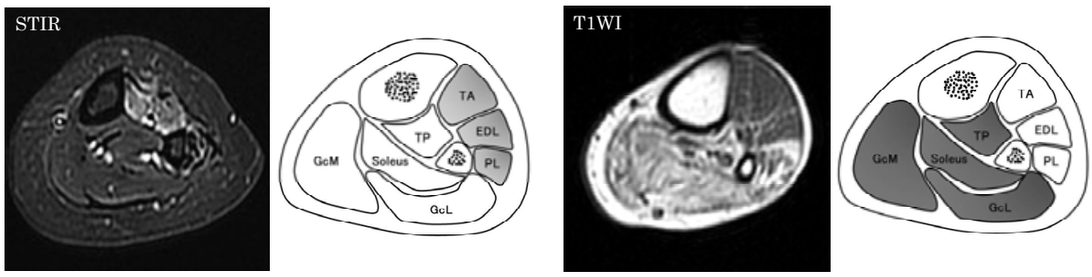
Case Presentation

Case 1: Common peroneal nerve palsy

A 21-year-old woman developed left foot weakness during the course of treatment for fulminant myocarditis in the intensive care unit. Neurological examination revealed weakness of left foot dorsiflexion 2/5 (MRC scale) and a tingling sensation was distributed on the left lateral leg and dorsal foot. MRI showed a high intensity signal in the TA, EDL and PL with STIR sequence (Fig. 2a), supporting the diagnosis of common peroneal nerve palsy.

Case 2: Tibial nerve palsy

A 52-year-old man, with a history of a left tibia fracture at the age of six, was referred to our hospital for the evaluation of his frequent stumbling. Neurological examination revealed weakness of plantar flexion and atrophy of the calf muscles on the left leg. MRI showed an increased T1 signal in the lateral and medial heads of the gastrocnemius (GC), soleus and tibialis posterior (TP) muscles (Fig. 2b). The MRI findings are compatible with the diagnosis of tibial mononeuropathy associated with tibial fracture.



a b

Abbreviations: extensor digitorum longus (EDL), gastrocnemius lateral head (GcL), gastrocnemius medial head (GcM), peroneus longus (PL), tibialis anterior (TA), tibialis posterior (TP).

Fig. 2. (a) Compression neuropathy of the common peroneal nerve. Axial MRI of the proximal part of the left leg with STIR sequence. (b) Tibial nerve palsy associated with tibia fracture. Axial T1-weighted MRI of the middle part of the left leg.

5.1.5 Sciatic nerve

The above two cases exemplify damages in the tibial and peroneal nerves (section 5.1.4), both of which are branches of the sciatic nerve. More proximal damage in the sciatic nerve may additionally involve the hamstring muscles. Causes of sciatic nerve neuropathy include trauma (e.g. dislocation of the hip joint and pelvic fracture), compression (e.g. tumour and metastatic lesions) and iatrogenic injury (e.g. in association with total hip replacement and intramuscular injection). Piriformis syndrome refers to compression of the sciatic nerve by the piriformis muscle. It induces sciatic pain and numbness in the buttocks, typically without weakness. The diagnosis of piriformis syndrome is often challenging because of limited sensitivity and specificity of physical signs and the absence of electrodiagnostic

criteria. Filler and colleagues demonstrated that unilateral T2 high intensity of the sciatic nerve at the sciatic notch and asymmetry of the piriformis muscle on the MRI are the findings specific to piriformis syndrome (Filler et al., 2005). No abnormalities of the sciatic-innervated muscles are seen on the MRI. Accurate diagnosis of piriformis syndrome is important because it may lead to surgical treatment for pain relief.

5.1.6 Femoral nerve

Causes of femoral neuropathy include compression (e.g. retroperitoneal haemorrhage often from excessive anticoagulation), stretch injuries (e.g. prolonged lithotomy position), surgical procedures (e.g. hip replacement), direct injuries (inguinal surgery and wounds), radiation injury, ischemia (common iliac artery occlusion) and diabetic amyotrophy (Kuntzer et al., 1997). MRI is useful for the evaluation of mass lesions compressing the femoral nerve (Seijo-Martinez et al., 2003; Stuplich et al., 2005). In case of radiation injury, MRI may show local fibrosis constricting the femoral nerve (Nogués et al., 1998). Femoral neuropathy presents, often acutely, with thigh weakness and numbness. Femoral nerve supplies the psoas major, iliacus, pectineus, sartorius and quadriceps femoris muscles. Muscles involved may vary, depending on the level of the nerve lesion. MRI has a potential to detect denervation signals in these muscles (Nogués et al., 1998; Carter et al., 1995).

5.2 Radiculopathy

Clinical symptoms of radiculopathy are characterized by pain and radiating paresthesia along the affected dermatomes and motor weakness of the affected myotomes. The common causes of radiculopathy are structural lesions, such as herniated disk, bony impingement from spondylosis and mass lesions, such as epidural abscess and metastatic tumour to the spine. Radiculopathy may also be caused by non-structural lesions, such as carcionomatous or lymphomatous meningitis, borreliosis and herpes zoster infection.

MRI is widely used to identify structural lesions causing radiculopathy. Bone and disk diseases most frequently affect the cervical (C4–8) and lumbosacral (L3–S1) segments. MRI findings of foraminal impingement and nerve root compression directly support the diagnosis of radiculopathy. MRI is also useful for visualization of the denervated muscles to confirm the involved myotomes. For example, MRI for patients with subacute lumbar radiculopathy may show a high STIR signal in the muscles of the affected root level, with which needle EMG findings of acute denervation closely correlate (Carter et al., 1997).

Foot drop is a typical situation in which MRI is useful for diagnosis. When foot drop is caused by L5 radiculopathy, MRI may reveal denervation signals in the anterior compartment muscles (TA, EDL and PL) and the TP muscle. A peroneal mononeuropathy may also cause weakness of the anterior compartment muscles (see also the section 5.1.4), but TP would not be involved because it is innervated by the tibial nerve. Thus, whether TP muscle is involved or not has a key diagnostic value in foot drop (Bendszus and Koltzenburg, 2001).

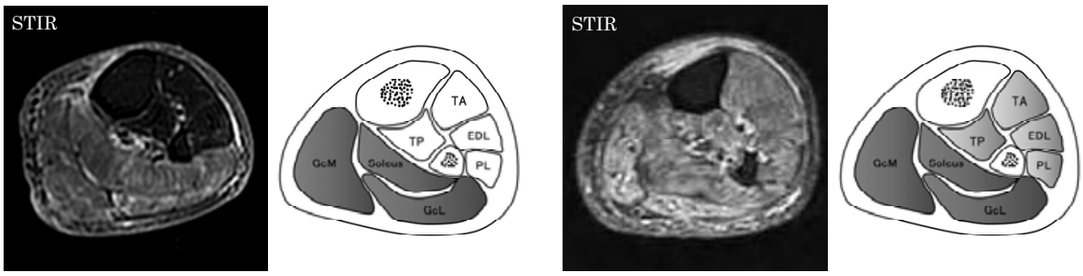
Case Presentation

Case 1: S1 radiculopathy

A 75-year-old man has been conservatively treated for lumbago, sciatica and intermittent claudication, caused by lumbar canal stenosis associated with intervertebral disk hernia at L4/5 and L5/S1 levels. Neurological examination revealed weakness of the left GC muscle with absent ankle jerk. Active neurogenic EMG changes and increased STIR signals were observed in the soleus and GC muscles (Fig. 3a), supporting the diagnosis of S1 radiculopathy.

Case 2: L5-S1 polyradiculopathy

A 53-year-old man experienced progressive weakness of the left lower extremity. He had a past history of lumbar spondylosis, which was surgically treated at the age 49. MRI showed high STIR signals in the muscles of L5 and S1 myotomes (TA, EDL, PL, TP, soleus and GC, Fig. 3b).



a b

Abbreviations: extensor digitorum longus (EDL), gastrocnemius lateral head (GcL), gastrocnemius medial head (GcM), peroneus longus (PL), tibialis anterior (TA), tibialis posterior (TP).

Fig. 3. Axial MRI (STIR) of the leg in two patients with S1 radiculopathy (a) and L5+S1 polyradiculopathy (b).

5.3 Polyneuropathy

Polyneuropathy is characterized by a distal symmetrical distribution of sensory motor deficits. Sensory loss occurs in a glove and stocking distribution, and motor weakness begins in the distal limbs. There are many causes of polyneuropathy, including nutritional deficiencies, immunological conditions, systemic metabolic disorders, toxins and hereditary disorders. The distal dominant distribution of the sensory motor symptoms may reflect a length-dependent process of dying-back axonopathy. Or it may reflect a demyelinating process, which also shows a length-dependent pattern because longer fibres have a higher probability of conduction block due to demyelination. Recent MRI studies have demonstrated the length-dependent pattern or centripetal progression of muscle denervation in both acquired (Andersen et al., 2004; Andreassen et al., 2009) and hereditary (Gallardo et al., 2006; Chung et al., 2008) forms of polyneuropathy.

Diabetic patients commonly develop sensory polyneuropathy with distal pain and sensory loss. Diabetic polyneuropathy also leads to denervation and loss of distal muscles. Andersen and colleagues estimated muscle volumes in patients with long-term diabetic polyneuropathy by using a stereological determination method based on cross-sectional T1-weighted MRI (Andersen et al., 2004). The volume of the intrinsic foot muscles was halved in diabetic patients with chronic neuropathy, in comparison with that of diabetic patients without neuropathy. The foot muscle volume was closely related to the compound muscle action potentials (CMAPs) of the peroneal nerve. Muscle atrophy occurs early in the feet and progresses steadily in the lower legs.

Distal dominant denervation also occurs in hereditary forms of polyneuropathy. Charcot-Marie-Tooth (CMT) disease is a pathologically and genetically heterogeneous polyneuropathy, divided into demyelinating type (e.g. CMT 1A) and axonal type (e.g. CMT 2A). Both CMT 1A and 2A are characterized by distal muscular atrophy and patients with minimal phenotype

may show fatty infiltration limited to intrinsic foot muscles on T1-weighted MRI (Berciano et al., 2010). This finding supports the notion that pes cavus, a cardinal manifestation of CMT, is associated with selective denervation of intrinsic foot muscles. Afterwards, weakness in the more proximal muscles progresses with variable severity. Interestingly, CMT 1A patients show denervation predominantly in the muscles supplied by the peroneal nerve: muscles in the anterior and lateral compartments show selective fatty infiltration with relative preservation of the posterior compartment muscles (Price et al., 1993; Gallardo et al., 2006; Chung et al, 2008). By contrast, in most of the late-onset CMT 2A patients, MRI shows preferential involvement of the soleus muscle with relatively spared deep posterior compartment muscles. The thigh muscles may also be involved during the advanced stage of CMT. A T1-weighted signal may be stronger on the distal side of the vastus lateralis and medialis muscles on coronal images (Chung et al., 2008; Berciano et al., 2010). In addition to T1 high signals that reflect fatty infiltration, T2 high signals and Gd enhancement were also reported in both CMT 1A and 2A patients (Gallardo et al., 2005; Chung et al., 2008). Because T2 prolongation and Gd enhancement are usually observed in acutely denervated muscles, it is difficult to interpret these findings in a chronic disorder with minimal clinical progression over decades. It might indicate subclinical active denervation, but future studies are needed to better understand the muscle MRI findings in CMT.

Case Presentation: CMT type 2

A 41-year-old man, who gradually developed gait disturbance since adolescence, was referred to our hospital for neurological evaluation. One of his uncles has similar gait disturbance. On neurological examination, he had distal-dominant weakness of the lower extremities and sensory loss in a glove and stocking distribution. A nerve conduction study showed decreased CMAP and sensory nerve action potential amplitudes with preserved conduction velocities in all examined nerves, indicating sensory motor axonal polyneuropathy. Clinical diagnosis of CMT type 2 was made. On coronal T2-weighted MRI, the GC muscle showed a high intensity signal with distal accentuation (arrowheads in Fig. 4a). A T1-weighted MRI showed fatty infiltration of the anterior, lateral and superficial posterior compartment muscles (Fig. 4b).



a b

Fig. 4. Muscle MRI of a patient with CMT type 2. (a) T2-weighted coronal (a) and T1-weighted axial (b) MRI of legs.

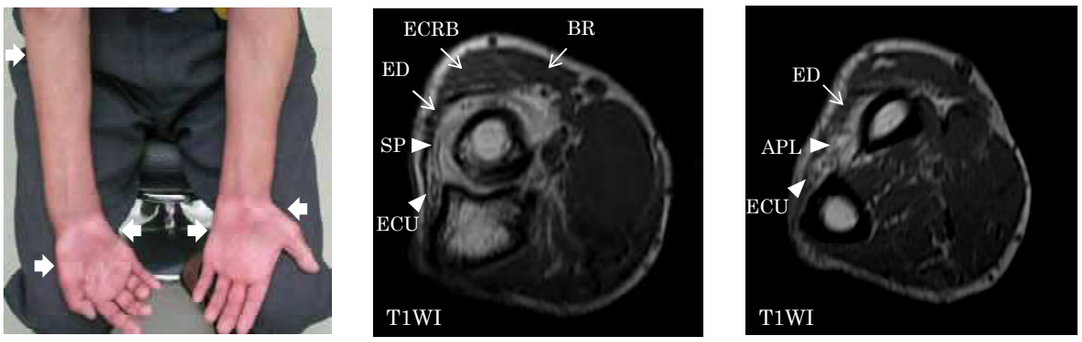
5.4 Mononeuropathy multiplex

Mononeuropathy multiplex is a clinical syndrome characterized by an asymmetric, stepwise progression of sensory motor deficits involving more than one peripheral or cranial nerve. Mononeuropathy multiplex is often associated with systemic or non-systemic vasculitis, including polyarteritis nodosa, rheumatoid arthritis, systemic lupus erythematosus, Churg-Strauss syndrome and Wegener's granulomatosis. The common peroneal nerve is affected in 75% of patients with vasculitic neuropathy, causing a painful foot drop.

Multifocal motor neuropathy (MMN) and multifocal acquired demyelinating sensory and motor neuropathy (MADSAM, or Lewis-Sumner syndrome) also show the clinical pattern of mononeuropathy multiplex, with electrophysiological evidence of demyelination and conduction block. Brachial plexus of MMN patients is known to show swelling and an increased signal on T2-weighted MRI (van Es et al., 1997). In a few cases, the high intensity signal has been shown to co-localize with conduction block (Parry, 1996). The Gd enhancement effect of the swollen nerve roots has also been described in MMN (Kaji et al., 1993; Perry, 1996). On the other hand, little is known about the muscle MRI findings in MMN. An example case of MMN presented below showed an increased T1 signal in the muscles associated with the nerves with conduction block.

Case Presentation: MMN

A 59-year old man gradually developed clumsiness of the right hand over 10 years. On neurological examination, he had asymmetric weakness of the upper limbs, especially bilateral intrinsic hand muscles and the right extensor muscles. Severe atrophy was present in the bilateral thenar, hypothenar and right brachioradialis muscles (Fig. 5a). There was no sensory deficit and all deep tendon reflexes were absent. Nerve conduction studies revealed multiple conduction blocks. Radial-innervated muscles showed marked atrophy with (SP, ECU, APL; arrowheads in Fig. 5b, c) or without (ED, ECRB, BR; arrows in Fig. 5b, c) signal change on T1-weighted MRI.



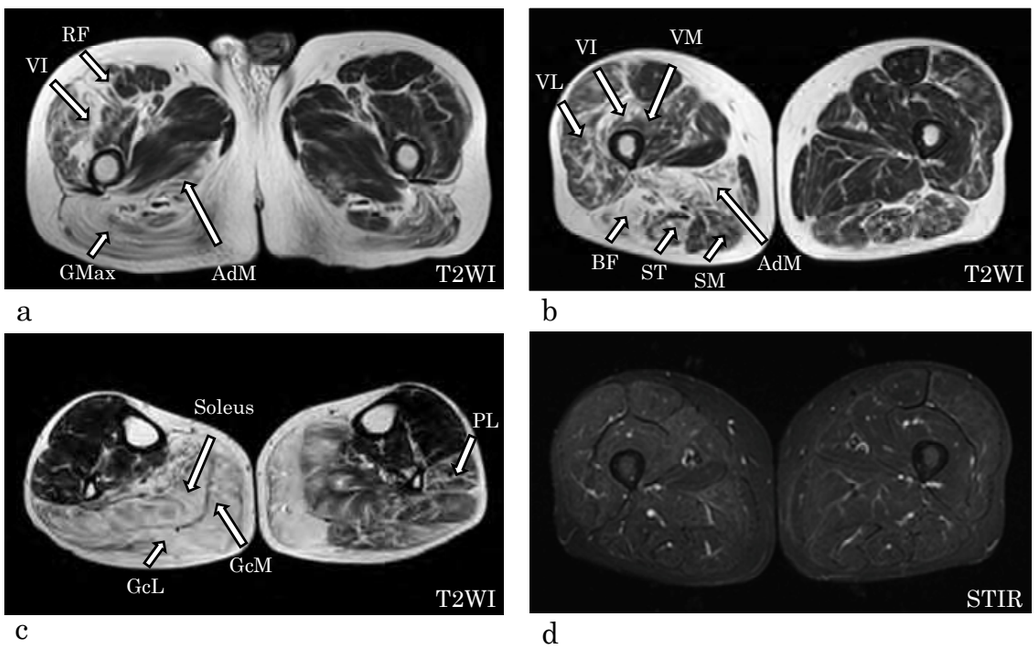
Abbreviations: abductor pollicis longus (APL), brachioradialis (BR), extensor carpi radialis brevis (ECRB), extensor carpi ulnaris (ECU), extensor digitorum (ED), supinator (SP).

Fig. 5. A case of multifocal motor neuropathy. (a) Muscle atrophy in the bilateral thenar, hypothenar and right brachioradialis muscles. (b, c) Axial T1-weighted muscle MRI of the right forearm.

5.5 Plexopathy

Brachial plexopathy causes pain, paresthesia and motor weakness in the distribution of nerve roots C5 to Th1. Common causes of brachial plexopathy include trauma, neoplastic infiltration, neuralgic amyotrophy, delayed radiation injury and thoracic outlet syndrome. Bilbey et al. showed that MRI is 63% sensitive and 100% specific in demonstrating the abnormality of the brachial plexus in a diverse patient population (Bilbey et al., 1994). When plexopathy is caused by a mass lesion, MRI can often determine whether the mass is intrinsic or extrinsic to the plexus. MRI is also useful for characterizing neoplastic processes (e.g. nerve sheath tumours, metastases, direct extension of non-neurogenic primary tumour and lymphoma) and benign processes (e.g. fibromatosis, lipoma, myositis ossificans, ganglioneuroma, hemangioma and lymphangioma) (Bowen and Seidenwurm, 2008).

Lumbosacral plexopathy is a relatively rare clinical entity that induces sensory motor deficits in the distribution of L1 to S3 segments, causing weakness and sensory loss in the territories of the obturator, femoral, gluteal (motor only), peroneal and tibial nerves. Common causes of lumbosacral plexopathy include trauma (e.g. pelvic fracture), diabetic amyotrophy, retroperitoneal haemorrhage, tumours and inflammation.



Abbreviations: adductor magnus (AdM), biceps femoris (BF), gastrocnemius lateral head (GcL), gastrocnemius medial head (GcM), gluteus maximus (GMax), peloneus longus (PL), rectus femoris (RF), semimenbranosus (SM), semitendinosus (ST), vastus intermedius (VI), vastus lateralis (VL), vastus medialis (VM).

Fig. 6. Post-irradiation lumbosacral pexopathy in a 50-year-old man. (a-c) Axial T2-weighted MRI of the hip (a), thigh (b) and leg (c). (d) STIR images of the thigh.

Muscle MRI findings of plexopathy have not been established yet. Several studies report muscle MRI findings in neuralgic amyotrophy, also known as Parsonage-Turner syndrome (Gaskin and Helms, 2006; Scalf et al., 2007). The most typical finding of neuralgic amyotrophy is diffuse high signal intensity on T2-weighted images involving one or more

muscles innervated by the brachial plexus. T1-weighted images may also show atrophy of the affected muscles. The supraspinatus and infraspinatus muscles, both innervated by the suprascapular nerve, are most frequently affected (>80%). Less frequently involved are the axillary-innervated deltoid and teres minor muscles. MRI has an advantage in that it can exclude other causes of shoulder pain, such as rotator cuff tear, impingement syndrome or labral tear.

Case Presentation: Post-irradiation lumbosacral plexopathy

A 50-year-old man gradually developed weakness of the bilateral legs over 10 years. He had a history of suprasellar germinoma at the age of 24, which went into complete remission after radiation and chemotherapy. On neurological examination, he showed weakness of the bilateral legs without sensory deficits. Needle EMG showed chronic neurogenic changes and myokimic discharges in the leg muscles, which supported the diagnosis of radiation-induced delayed lumbosacral plexopathy.

T1- and T2-weighted MRI showed an asymmetric high intensity signal in the hip, thigh and calf muscles (arrows in Fig. 6a-c). The involved muscles showed isointensity signals on STIR images (Fig. 6d). Taken together, the MRI study was compatible with the idea of chronic-stage denervation in the distribution of lumbosacral plexopathy.

6. Conclusion

We reviewed the clinical utility of muscle MRI on a variety of peripheral nerve disorders. MRI has reasonable sensitivity for detecting denervated muscles. Future improvement of scan sequences and availability of higher field scanners would make the sensitivity even higher. Yet, its disease specificity is limited and MRI plays a complementary role in the diagnosis of peripheral nerve disorders.

7. References

Andersen H.; Gjerstad M.D. and Jakobsen J. (2004). Atrophy of foot muscles: a measure of diabetic neuropathy. *Diabetes Care*, Vol.27, No.10, (October 2004), pp. 2382-2385

Andreassen C.S.; Jakobsen J.; Ringgaard S.; Ejskjaer N. and Andersen H. (2009). Accelerated atrophy of lower leg and foot muscles--a follow-up study of long-term diabetic polyneuropathy using magnetic resonance imaging (MRI). *Diabetologia*, Vol.52, No.6, (January 2009), pp. 1182-1191

Andreisek G.; Crook D.W.; Burg D.; Marincek B. and Weishaupt D. (2006). Peripheral neuropathies of the median, radial and ulnar nerves: MR imaging features. *Radiographics*, Vol.26, No.5, (September-October 2006), pp. 1267-1287

Berciano J.; Gallardo E.; García A.; Ramón C.; Infante J. and Combarros O. (2010). Clinical progression in Charcot-Marie-Tooth disease type 1A duplication: clinico-electrophysiological and MRI longitudinal study of a family. *J Neurol*, Vol.257, No.10, (October 2010), pp. 1633-1641

Bendszus M. and Koltzenburg M. (2001). Visualization of denervated muscle by gadolinium-enhanced MRI. *Neurology*. Vol.57, No.9, (November 2001), pp. 1709-1711

Bendszus M.; Koltzenburg M.; Wessig C.; Solymosi L. (2002). Sequential MR imaging of denervated muscle: experimental study. *Am J Neuroradiol*, Vol.23, No.8, (September 2002), pp. 1427-1431

Bendszus M.; Wessig C.; Reiners K.; Bartsch A.J.; Solymosi L. and Koltzenberg M. (2003). MR imaging in the differential diagnosis of neurogenic foot drop. *Am J Neuroradiol*, Vol.24, No.7, (August 2003), pp. 1283-1289

Bilbey J.H.; Lamond R.G. and Mattrey R.F. (1994). MR imaging of disorders of the brachial plexus. *J Magn Reson Imaging*, Vol.4, No.1. (January-February 1994), pp. 13-18

Bowen B.C. and Seidenwurm D.J. (2008). Plexopathy. *Am J Neuroradiol*, Vol.29, No.2, (February 2008), pp.400-402

Carter G.T. and Fritz R.C. (1997). Electromyographic and lower extremity short time to inversion recovery magnetic resonance imaging findings in lumbar radiculopathy. *Muscle Nerve*, Vol.20, No.9, (September 1997) pp. 1191-1193

Carter G.T.; McDonald C.M.; Chan T.T. and Margherita A.J. (1995). Isolated femoral mononeuropathy to the vastus lateralis: EMG and MRI findings. *Muscle Nerve*, Vol.18, No.3, (March 1995), pp. 341-344

Chung K.W.; Suh B.C.; Shy M.E.; Cho S.Y.; Yoo J.H.; Park S.W.; Moon H.; Park K.D.; Choi K.G.; Kim S.; Kim S.B.; Shim D.S.; Kim S.M.; Sunwoo I.N. and Choi B.O. (2008). Different clinical and magnetic resonance imaging features between Charcot-Marie-Tooth disease type 1A and 2A. *Neuromuscul Disord*, Vol.18, No.8, (August 2008), pp. 610-618

Donovan A.; Rosenberg Z.S. and Cavalcanti C.F. (2010) MR imaging of entrapment neuropathies of the lower extremity. Part 2. The knee, leg, ankle and foot. *Radiographics*, Vol.30, No.4, (July-August 2010), pp. 1001-1019

Ferdinand B.D.; Rosenberg Z.S.; Schweitzer M.E.; Stuchin S.A.; Jazrawi L.M.; Lenzo S.R.; Meislin R.J. and Kiprovski K. MR imaging features of radial tunnel syndrome: initial experience. *Radiology*, Vol.240, No.1, (July 2006), pp. 161-168

Filler A.G.; Haynes J.; Jordan S.E.; Prager J.; Villablanca J.P.; Farahani K.; McBride D.Q.; Tsuruda J.S.; Morisoli B.; Batzdorf U. and Johnson J.P. (2005). Sciatica of non-disc origin and piriformis syndrome: diagnosis by magnetic resonance neurography and interventional magnetic resonance imaging with outcome study of resulting treatment. *J Neurosurg Spine*, Vol.2, No.2, (February 2005), pp. 99-115

Filler A.G.; Howe F.A.; Hayes C.E.; Kliot M.; Winn H.R.; Bell B.A.; Griffiths J.R. and Tsuruda J.S. (1993). Magnetic resonance neurography. *Lancet*, Vol.341, No.8846, (March 1993), pp. 659-661

Fleckenstein J.L.; Watumull D.; Conner K.E.; Ezaki M.; Greenlee R.G.Jr.;Bryan W.W.; Chason D.P.; Parkey R.W.; Peshock R.M. and Purdy P.D. (1993). Denervated human skeletal muscle: MR imaging evaluation. *Radiology*, Vol.187, No.1, (April 1993), pp. 213-218

Gallardo E.; García A.; Combarros O. and Berciano J. (2006). Charcot-Marie-Tooth disease type 1A duplication: spectrum of clinical and magnetic resonance imaging features in leg and foot muscles. *Brain*, Vol.129, No.2, (February 2006), pp. 426-437

Gaskin C.M. and Helms C.A. (2006). Parsonage-Turner syndrome: MR imaging findings and clinical information of 27 patients. *Radiology*, Vol.240, No.2, (August 2006), pp. 501-507

Grainger A.J.; Campbell R.S. and Stothard J. (1998). Anterior interosseous nerve syndrome: appearance at MR imaging in three cases. *Radiology*, Vol.208, No.2, (August 1998), pp. 381-384

Grant G.A.; Britz G.W.; Goodkin R.; Jarvik J.G.; Maravilla K. and Kliot M. (2002). The utility of magnetic resonance imaging in evaluating peripheral nerve disorders. *Muscle Nerve*, Vol.25, No.3, (March 2002), pp. 314-331

Gyftopoulos S.; Rosenberg Z.S. and Petchprapa C. (2010). Increased MR signal intensity in the pronator quadratus muscle: does it always indicate anterior interosseous neuropathy? *Am J Roentgenol*, Vol.194, No.2, (February 2010), pp. 490-493

Hayashi Y.; Ikata T.; Takai H.; Takata S.; Ishikawa M.; Sogabe T. and Koga K. (1997). Effect of peripheral nerve injury on nuclear magnetic resonance relaxation times of rat skeletal muscle. *Invest Radiol*, Vol.32, No.3, pp. 135-139

Hazlewood C.F.; Chang D.C.; Nichols B.L. and Woessner D.E. (1974). Nuclear magnetic resonance transverse relaxation times of water protons in skeletal muscle. *Biophys J*, Vol. 14, No.8, (August 1974), pp. 582-606

Hof J.J.; Kliot M.; Slimp J. and Haynor D.R. (2008). What's new in MRI of peripheral nerve entrapment? *Neurosurg Clin N Am* , Vol.14, No.4, (October 2008), pp. 583-595

Horch R.E.; Allmann K.H.; Laubenberger J.; Langer M. and Stark G.B. (1997). Median nerve compression can be detected by magnetic resonance imaging of the carpal tunnel. *Neurosurgery*, Vol.41, No.1, (July 1997), pp. 76-82

Iverson D.J. (2005). MRI detection of cysts of the knee causing common peroneal neuropathy. *Neurology*, Vol.65, No.11, (December 2005), pp. 1829-1831

Jarvik J.G.; Yuen E.; Haynor D.R.; Bradley C.M.; Fulton-Kehoe D.; Smith-Weller T.; Wu R.; Kliot M.; Kraft G.; Wang L.; Erlich V.; Heagerty P.J. and Franklin G.M. (2002). MR nerve imaging in a prospective cohort of patients with suspected carpal tunnel syndrome. *Neurology*, Vol.58, No.11, (June 2002), pp. 1597-1602

Jonas D.; Conrad B.; Von Einsiedel H.G. and Bischoff C. (2000). Correlation between quantitative EMG and muscle MRI in patients with axonal neuropathy. *Muscle Nerve*, Vol.23, No.8, (August 2000), pp. 1265-1269

Kaji R.; Oka N.; Tsuji T.; Mezaki T.; Nishio T.; Akiguchi I. and Kimura J. (1993). Pathological findings at the site of conduction block in multifocal motor neuropathy. *Ann Neurol*, Vol.33, No.2, (February 1993), pp. 152-158

Kamath S.; Venkatanarasimha N.; Walsh M.A and Hughes P.M. (2008). MRI appearance of muscle denervation. *Skeletal Radiol*, Vol.37, No.5, (May 2008), pp. 397-404

Kato H.; Hirayama T.; Minami A.; Iwasaki N. and Hirachi K. (2002). Cubital tunnel syndrome associated with medial elbow Ganglia and osteoarthritis of the elbow. *J Bone Joint Surg Am*, Vol.84-A, No.8, (August 2002), pp. 1413-1419

Kikuchi Y.; Nakamura T.; Takayama S.; Horiuchi Y. and Toyama Y. (2003). MR imaging in the diagnosis of denervated and reinnervated skeletal muscles: experimental study in rats. *Radiology*, Vol.229, No.3, (December 2003), pp. 861-867

Kim J.Y.; Ihn Y.K.; Kim J.S.; Chun K.A.; Sung M.S. and Cho K.H. (2007). Non-traumatic peroneal nerve palsy: MRI findings. *Clin Radiol*, Vol.62, No.1, (January 2007), pp. 58-64

Kim S.J.; Hong S.H.; Jun W.S.; Choi J.Y.; Myung J.S.; Jacobson J.A.; Lee J.W.; Choi J.A.; Kan and H.S. (2011). MR imaging mapping of skeletal muscle denervation in entrapment and compressive neuropathies. *Radiographics*, Vol.31, No.2, (March-April 2011), pp. 319-332

Koltzenburg M.; Bendszus M. (2004). Imaging of peripheral nerve lesions. *Curr Opin Neurol*, Vol.17, No.5, (October 2004), pp. 621-626

Kuntzer T.; van Melle G. and Regli F. (1997). Clinical and prognostic features in unilateral femoral neuropathies. *Muscle Nerve*, Vol.20, No.2, (February 1997), pp. 205-211.

Lisle D.A.; Johnstone S.A. (2007). Usefulness of muscle denervation as an MRI sign of peripheral nerve pathology. *Australas Radiol*, Vol.51, No.6, (December 2007), pp. 516-526

McDonald C.M.; Carter G.T.; Fritz R.C.; Anderson M.W.; Abresch R.T. and Kilmer D.D. (2000). Magnetic resonance imaging of denervated muscle: comparison to electromyography. *Muscle Nerve*, Vol.23, No.9, (September 2000), pp. 1431-1434

Mesgarzadeh M.; Schneck C.D.; Bonakdarpour A.; Mitra A. and Conaway D. (1989) Carpal tunnel: MR imaging. Part II. Carpal tunnel syndrome. *Radiology*, Vol.171, No.3, (June 1989), pp. 749-754.

Nogués M.A.; Salas E.; Martínez A. and Romero C. (1998). Unilateral femoral neuropathy. *Muscle Nerve*, Vol.21, No.1, (January 1998), pp. 126-127

Parry GJ. (1996). AAEM case report #30: multifocal motor neuropathy. *Muscle Nerve*, Vol.19, No.3, pp. 269-276

Pearce C.; Feinberg J. and Wolfe S.W. (2009). Ulnar neuropathy at the wrist. *HSSJ*, Vol.5, No.2, (September 2009), pp. 180-183

Petchprapa C.N.; Rosenberg Z.S.; Sconfienza L.M.; Cavalcanti C.F.; Vieira R.L. and Zember J.S. (2010). MR imaging of entrapment neuropathies of the lower extremity. Part 1. The pelvis and hip. *Radiographics*, Vol.30, No.4, (July-August 2010), pp. 983-1000

Polak J.F.; Jolesz F.A. and Adams D.F. (1988). Magnetic resonance imaging of skeletal muscle. Prolongation of T1 and T2 subsequent to denervation. *Invest Radiol*, Vol.23, No.5, (May 1988), pp. 365-369

Price A.E.; Maisel R. and Drennan J.C. Computed tomographic analysis of pes cavus. (1993). *J Pediatr Orthop*, Vol.13, No.5, (September 1993), pp. 646-653

Rinker B.; Effron C.R. and Beasley R.W. (2004). Proximal radial compression neuropathy. *Ann Plast Surg*, Vol.52, No.2, (February 2004), pp. 174-180

Rosenberg Z.S.; Beltran J.; Cheung Y.Y.; Ro S.Y.; Green S.M. and Lenzo S.R. (1993). The elbow: MR features of nerve disorders. *Radiology*, Vol.188, No.1, (July 1993), pp. 235-240

Sallomi D.; Janzen D.L.; Munk P.L.; Connell D.G. and Tirman P.F. (1998). Muscle denervation patterns in upper limb nerve injuries: MR imaging findings and anatomic basis. *Am J Roentgenol*, Vol.171, No.3, (September 1998), pp. 779-784

Scalf R.E.; Wenger D.E.; Frick M.A.; Mandrekar J.N. and Adkins M.C. (2007). MRI findings of 26 patients with Parsonage-Turner syndrome. *Am J Roentgenol*, Vol.189, No.1, (July 2007), pp. W39-44

Seijo-Martínez M.; Castro del Río M.; Fontoira E. and Fontoira M. (2003). Acute femoral neuropathy secondary to an iliacus muscle hematoma. *J Neurol Sci*, Vol.209, No.1-2, (May 2003), pp. 119-122

Shabas D.; Gerard G. and Rossi D. (1987). Magnetic resonance imaging examination of denervated muscle. *Comput Radiol*, Vol.11, No.1, (January-February 1987), pp. 9-13

Spratt J.D.; Stanley A.J.; Grainger A.J.; Hide I.G. and Campbell R.S. (2002). The role of diagnostic radiology in compressive and entrapment neuropathies. *Eur Radiol*, Vol.12, No.9, (September 2002), pp. 2352-2364

Stoll G.; Bendszus M.; Perez J. and Pham M. (2009). Magnetic resonance imaging of the peripheral nervous system. *J Neurol*, Vol.256, No.7, (July, 2009), pp. 1043-1051

Stuplich M.; Hottinger A.F.; Stoupis C. and Sturzenegger M. (2005). Combined femoral and obturator neuropathy caused by synovial cyst of the hip. *Muscle Nerve*, Vol.32, No.4, (October 2005), pp. 552-554

Takahara T.; Hendrikse J.; Yamashita T.; Mali W.P.; Kwee T.C. Imai Y. and Luijten P.R. (2008). Diffusion-weighted MR neurography of the brachial plexus: feasibility study. *Radiology*, Vol.249, No.2, (November 2008), pp. 653-660

Thawait S.K.; Wang K.; Subhawong T.K.; Williams E.H.; Hashemi S.S.; Machado A.J.; Thawait G.K.; Soldatos T.; Carrino J.A. and Chhabra A. (2011). Peripheral nerve surgery: the role of high-resolution MR neurography. *Am J Neuroradiol*, (April 2011), [Epub ahead of print], DOI 10.3174/ajnr.A2465

Tsujii M.; Hirata H.; Morita A. and Uchida A. (2009). Palmar bowing of the flexor retinaculum on wrist MRI correlates with subjective reports of pain in carpal tunnel syndrome. J *Magn Reson Imaging*, Vol.29, No.5, (May 2009), pp. 1102-1105

Uetani M.; Hayashi K.; Matsunaga N.; Imamura K. and Ito N. (1993). Denervated skeletal muscle: MR imaging. Work in progress. *Radiology*. Vol. 189, No.2, (November 1993), pp. 511-515

Van Es H.W.; Van den Berg L.H.; Franssen H.; Witkamp T.D.; Ramos L.M.; Notermans N.C.; Feldberg M.A. and Wokke J.H. (1997). Magnetic resonance imaging of the brachial plexus in patients with multifocal motor neuropathy. *Neurology*, Vol.48, No.5, (May 1997), pp. 1218-1224

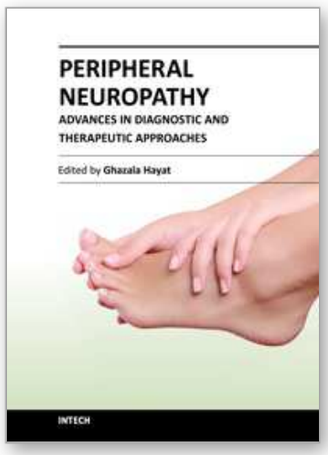
Wessig C.; Koltzenburg M.; Reiners K.; Solymosi L. and Bendszus M. (2004). MRI of peripheral nerve degeneration and regeneration: correlation with electrophysiology and histology. *Exp Neurol*, Vol.188, No.1, (July 2004), pp. 171-177

West G.A.; Haynor D.R.; Goodkin R.; Tsuruda J.S.; Bronstein A.D.; Kraft G.; Winter T. and Kliot M. (1994). Magnetic resonance imaging signal changes in denervated muscles after peripheral nerve injury. *Neurosurgery*, Vol.35, No.6, (December 1994), pp. 1077-1086

Zhang Z.; Song L.; Meng Q.; Li Z.; Pan B.; Yang Z. and Pei Z. (2009). Morphological analysis in patients with sciatica: a magnetic resonance imaging study using three-dimensional high-resolution diffusion-weighted magnetic resonance neurography techniques. *Spine*, Vol.34, No.7, (April 2009), pp. E245-250

IntechOpen

IntechOpen



Peripheral Neuropathy - Advances in Diagnostic and Therapeutic Approaches

Edited by Dr. Ghazala Hayat

ISBN 978-953-51-0066-9
Hard cover, 206 pages
Publisher InTech
Published online 29, February, 2012
Published in print edition February, 2012

Over the last two decades we have seen extensive progress within the practice of neurology. We have refined our understanding of the etiology and pathogenesis for both peripheral and central nervous system diseases, and developed new therapeutic approaches towards these diseases. Peripheral neuropathy is a common disorder seen by many specialists and can pose a diagnostic dilemma. Many etiologies, including drugs that are used to treat other diseases, can cause peripheral neuropathy. However, the most common cause is Diabetes Mellitus, a disease all physicians encounter. Disability due to peripheral neuropathy can be severe, as the patients suffer from symptoms daily. This book addresses the advances in the diagnosis and therapies of peripheral neuropathy over the last decade. The basics of different peripheral neuropathies is briefly discussed, however, the book focuses on topics that address new approaches to peripheral neuropathies.

How to reference
In order to correctly reference this scholarly work, feel free to copy and paste the following:

Nozomu Matsuda, Shunsuke Kobayashi and Yoshikazu Ugawa (2012). Role of Skeletal Muscle MRI inPeripheral Nerve Disorders, Peripheral Neuropathy - Advances in Diagnostic and Therapeutic Approaches, Dr. Ghazala Hayat (Ed.), ISBN: 978-953-51-0066-9, InTech, Available from: http://www.intechopen.com/books/peripheral-neuropathy-advances-in-diagnostic-and-therapeutic-approaches/role-of-skeletal-muscle-mri-inperipheral-nerve-disorders

INTECH
open science | open minds

InTech Europe
University Campus STeP Ri
Slavka Krautzeka 83/A
51000 Rijeka, Croatia
Phone: +385 (51) 770 447
Fax: +385 (51) 686 166
www.intechopen.com

InTech China
Unit 405, Office Block, Hotel Equatorial Shanghai
No.65, Yan An Road (West), Shanghai, 200040, China
中国上海市延安西路65号上海国际贵都大饭店办公楼405单元
Phone: +86-21-62489820
Fax: +86-21-62489821

© 2012 The Author(s). Licensee IntechOpen. This is an open access article distributed under the terms of the Creative Commons Attribution 3.0 License, which permits unrestricted use, distribution, and reproduction in any medium, provided the original work is properly cited.

IntechOpen

IntechOpen